JOURNAL OF AIRCRAFT
Vol. 36, No. 2, March–April 1999

Flight Test of Optimal Inputs and Comparison with Conventional Inputs

Eugene A. Morelli*
NASA Langley Research Center, Hampton, Virginia 23681-0001

A technique for designing optimal inputs for aerodynamic parameter estimation was flight tested on the F-18 High Alpha Research Vehicle. Model parameter accuracies calculated from flight-test data were compared on an equal basis for optimal input designs and conventional inputs at the same flight condition. In spite of errors in the a priori input design models and distortions of the input forms by the feedback control system, analysis of data generated by the optimal inputs revealed lower estimated parameter errors compared with conventional 3-2-1-1 and doublet inputs. In addition, the tests using optimal input designs demonstrated enhanced design flexibility, allowing the optimal input design technique to use a larger input amplitude to achieve further increases in estimated parameter accuracy without departing from the desired flight-test condition. This work validated the analysis used to develop the optimal input designs, and demonstrated the feasibility and effectiveness of the optimal input design technique.

Nomenclature

A, B, C, D = system matrices
a_y, a_z = linear accelerations, g
$\mathcal{D}$ = dispersion matrix
$E\{\ \}$ = expectation operator
J = cost function
L, M, N = body axis aerodynamic moments
M = information matrix
N = total number of sample times
n_i, n_s, n_o = dimension of the control, state, and output vectors
n_p = dimension of the parameter vector
p, q, r = body axis angular rates, rad/s
R = discrete noise covariance matrix
$S(i)$ = output sensitivity matrix at time $i\Delta t$
T = maneuver duration, s
Tr = trace
$\boldsymbol{u}$ = n_i-dimensional control vector
V = airspeed, ft/s
$\boldsymbol{x}$ = n_s-dimensional state vector
Y, Z = body axis aerodynamic forces
$\boldsymbol{y}$ = n_o-dimensional output vector
$\boldsymbol{y}(i)$ = output vector at time $i\Delta t$
$\boldsymbol{z}(i)$ = measured output vector at time $i\Delta t$
α = angle of attack, rad
β = sideslip angle, rad
Δt = sampling interval, s
δa = aileron deflection, rad
$\delta a\ sym$ = symmetric aileron deflection, rad
δf = trailing-edge flap deflection, rad
δ_{ij} = Kronecker delta
δr = rudder deflection, rad
δs = stabilator deflection, rad
Θ = pitch angle, rad
$\boldsymbol{\theta}$ = n_p-dimensional parameter vector
θ_j = jth model parameter
μ_j = jth input amplitude constraint
$\boldsymbol{\nu}(i)$ = measurement noise vector at time $i\Delta t$
ξ_k = kth output amplitude constraint
σ_j = jth estimated parameter standard error
ϕ = roll angle, rad

Subscript
0 = average or trim value

Superscripts
T = transpose
-1 = matrix inverse
$\hat{}$ = estimate

Introduction

EXPERIMENT design is important for identifying mathematical models of modern aircraft dynamics from flight-test data. The flight-test maneuver (equivalently, the flight-test input) has a major impact on the quality of the data for modeling purposes. A good experiment design must account for practical constraints during the flight test, while maximizing information contained in the data from expensive flight-test time.

The overall goal is to design an experiment that produces data from which model parameters can be estimated accurately. This translates into exciting the system modes so that the sensitivities of the model outputs to the parameters are high and correlations among the parameters are low. Frequency sweep inputs[1] can be used to do this, requiring little more than knowledge of the frequency range of interest for the modeling. This technique is restricted to moving a single input at a time, so off-axis responses or coupled motions are generally not well modeled from frequency sweep data. Frequency sweeps also require relatively long maneuver times, i.e., 1–2 min, to run through the frequency range of interest. Low-frequency components of the frequency sweep contribute to long maneuver times, and also increase the tendency for the aircraft to depart from the desired flight-test condition. For high-performance aircraft, limited flight-test time, multiple control effectors, and flight conditions such as high angle of attack make the frequency sweep approach expensive and difficult to use.

An alternate approach is to take advantage of a priori knowledge about the dynamics of the aircraft to focus the input energy at frequencies near the system modes. An a priori model

Received Nov. 9, 1997; revision received Aug. 4, 1998; accepted for publication Aug. 16, 1998.

*Research Engineer, Dynamics and Control Branch, Flight Dynamics and Control Division, M/S 132. Senior Member AIAA.

can be assembled using wind tunnel aerodynamic data and knowledge of rigid-body dynamics. This permits the design of short flight-test maneuvers with high information content that can be analyzed using maximum likelihood parameter estimation in the time domain.[2,3] A paradox occurs here, in that very good inputs will be designed when the a priori model is very good; however, in this case the experiment is less needed. Obviously, the input design technique must be robust to errors in the a priori model.

Designing an input for accurate model parameter estimation requires rich excitation of the system, which is frequently at odds with various practical constraints. One such practical constraint is the requirement that output amplitude excursions, e.g., in angle of attack or sideslip angle, about the flight-test condition be limited to assure the validity of an assumed model structure. Input amplitudes must be constrained for the same reason, and to avoid nonlinearities such as mechanical stops and rate limiting when the model is linear.

Designing an input that excites the aircraft dynamic response as much as possible when modal frequencies are imperfectly known, while simultaneously satisfying practical constraints, is a difficult problem. Several researchers have studied the problem of finding optimal inputs for aircraft parameter estimation.[4-13] The most serious obstacles to using the results of these studies in flight have been practical implementation issues. These include unrealizable optimal input forms, and failure to account for closed-loop control, actuator dynamics, or constraints on input and output amplitudes. Computationally, the difficulties have been the selection of an appropriate optimality criterion, inadequate numerical optimization techniques for finding global optimal solutions, and difficulties associated with multiple input design.

Recent research[14-16] has produced an optimal input design technique that addresses the preceding issues. The technique generates square wave inputs that are globally optimal in the sense that information content in the data is maximized for a fixed flight-test time, or, alternatively, specified parameter accuracy goals are achieved in minimum flight-test time.

The optimal input design technique has been shown to be theoretically sound,[14,15] has been validated in flight for aerodynamic model parameter estimation experiments using pilot implementation,[16] has been used successfully to specify flight-test maneuvers for closed-loop model identification at high angles of attack,[17] and has compared favorably with other techniques in the literature for a standard test problem.[18] In the latter reference, the global optimal square wave input produced the lowest value of the sum of estimated parameter variances, even though the maneuver time allotted for the optimal square wave input design was the smallest of any of the techniques studied (see Table 3 of Ref. 18, p. 281). This fact, though not pointed out by the authors of Ref. 18, demonstrates the effectiveness of the optimal input design technique.

The purpose of this work was to test the optimal input design technique in flight using a computerized system to implement the optimal inputs, and to compare flight-test results from the optimal inputs with results from conventional 3-2-1-1 and doublet inputs similarly implemented. The 3-2-1-1 input form has been shown to be very effective for aircraft parameter estimation in previous flight-test investigations.[11,12]

The next section outlines the theory involved in the optimal input design technique. Next, the F-18 High Alpha Research Vehicle (HARV) test aircraft is described, along with some details of the flight-test procedure. Following this, results from flight tests are presented and discussed.

Theoretical Development

Airplane dynamics can be described by the following linear model equations:

$$\dot{\boldsymbol{x}}(t) = A\boldsymbol{x}(t) + B\boldsymbol{u}(t) \tag{1}$$

$$\boldsymbol{x}(0) = \boldsymbol{x}_0 \tag{2}$$

$$\boldsymbol{y}(t) = C\boldsymbol{x}(t) + D\boldsymbol{u}(t) \tag{3}$$

$$\boldsymbol{z}(i) = \boldsymbol{y}(i) + \boldsymbol{v}(i), \qquad i = 1, 2, \ldots, N \tag{4}$$

The measurement noise $\boldsymbol{v}(i)$ is assumed Gaussian with

$$E\{\boldsymbol{v}(i)\} = \boldsymbol{0} \quad \text{and} \quad E\{\boldsymbol{v}(i)\boldsymbol{v}^T(j)\} = R\delta_{ij} \tag{5}$$

Nonlinear models can be used in Eqs. (1) and (3) without any modification in the following development of the optimal input design procedure. Linear models are used in Eqs. (1) and (3) because of the common practice of estimating stability and control derivatives from flight-test data, and for consistency with the data analysis to be given later.

The input quantities were control-surface deflections, with output quantities from air data (α, β); body-axis angular velocities (p, q, r); Euler angles (ϕ); and translational accelerations (a_y, a_z). Longitudinal and lateral cases were treated separately, with the linear model structure shown earlier resulting from the usual small perturbation assumptions.[2]

Constraints arising from practical flight-test considerations were imposed on all input amplitudes and selected output amplitudes. Control-surface amplitudes are limited by mechanical stops, flight control software limiters, or linear control effectiveness. Selected output amplitudes must be limited to avoid departure from the desired flight-test condition and to ensure validity of the assumed linear model structure. In addition, constraints may be required on aircraft attitude angles for flight-test operational considerations, such as flight safety and maintaining line of sight from the data downlink antenna aboard the aircraft to the ground station. The constraints were specified by

$$|u_j(t) - u_{j_0}| \le \mu_j \quad \forall\, t, \qquad j = 1, 2, \ldots, n_i \tag{6}$$

$$|y_k(t) - y_{k_0}| \le \xi_k \quad \forall\, t, \qquad k \in (1, 2, \ldots, n_o) \tag{7}$$

where μ_j and ξ_k were positive constants, and y_{k_0} was the trim value of y_k, etc.

When estimating model parameter values from measured data, the minimum achievable parameter standard errors using an asymptotically unbiased and efficient estimator (such as maximum likelihood) are called the Cramér–Rao lower bounds.[2,3,14] These quantities are a function of the excitation of the system and the noise levels, and collectively measure the information content in the data. For a fixed instrumentation system, the Cramér–Rao lower bounds are influenced by the excitation of the system, which is determined by the input. The input implicitly includes the length of the maneuver.

The Cramér–Rao lower bounds for the parameter standard errors are given by the square root of the diagonal elements of the dispersion matrix $\mathcal{D}$.[2,3,14] The dispersion matrix is defined as the inverse of the information matrix M, the latter being a measure of the information content of the data from an experiment. The expressions for these matrices are

$$M = \sum_{i=1}^{N} S(i)^T R^{-1} S(i) \tag{8}$$

$$\mathcal{D} = M^{-1} \tag{9}$$

where $S(i)$ is the matrix of output sensitivities to the parameters

$$S(i) = \left.\frac{\partial \boldsymbol{y}(i)}{\partial \boldsymbol{\theta}}\right|_{\boldsymbol{\theta}=\hat{\boldsymbol{\theta}}} \tag{10}$$

and $\hat{\boldsymbol{\theta}}$ denotes the parameter vector estimate. The output sensitivities for the jth parameter appear as the jth column of the sensitivity matrix, and are computed from

$$\frac{d}{dt}\left(\frac{\partial \boldsymbol{x}}{\partial \theta_j}\right) = A\frac{\partial \boldsymbol{x}}{\partial \theta_j} + \frac{\partial A}{\partial \theta_j}\boldsymbol{x} + \frac{\partial B}{\partial \theta_j}\boldsymbol{u} \tag{11}$$

$$\frac{\partial \boldsymbol{x}}{\partial \theta_j}(0) = \boldsymbol{0} \tag{12}$$

$$\frac{\partial \boldsymbol{y}}{\partial \theta_j} = C\frac{\partial \boldsymbol{x}}{\partial \theta_j} + \frac{\partial C}{\partial \theta_j}\boldsymbol{x} + \frac{\partial D}{\partial \theta_j}\boldsymbol{u} \tag{13}$$

for $j = 1, 2, \ldots, n_p$. Equations (11–13) follow from differentiating Eqs. (1–3) with respect to θ_j, combined with the assumed analyticity of $\boldsymbol{x}$ for the model equations. The output sensitivities $S(i)$ can also be computed using finite differences and Eqs. (1–3).

From Eqs. (8–13), it is clear that the information matrix elements (and, therefore, the Cramér–Rao bounds) depend on the input through the sensitivity equations (11–13). The input $\boldsymbol{u}$ influences the sensitivities both directly as a forcing function in the sensitivity equations and indirectly as an influence on the states, which also force the sensitivity equations. The dependence of the Cramér–Rao bounds on the input is nonlinear in the input amplitude, regardless of whether or not the system equations (1) and (3) are linear, because of the nonlinear character of Eqs. (8) and (9).

Equation (8) is a discrete approximation to a time integral over the maneuver duration $T = N\Delta t$. Therefore, when comparing the effectiveness of various input designs using some function of $\mathcal{D}$ as the criterion for comparison, the input designs being compared should have the same maneuver duration and, in light of the last paragraph, also the same allowable maximum input amplitude. This approach contrasts with comparisons presented in previous works,[11,12,18] which were based on constant input energy. If only constant input energy is imposed on all inputs, a comparison made using a criterion that is a function of $\mathcal{D}$ is unfair because a wide range of maximum allowable input amplitudes and maneuver durations can give the same input energy. The inputs compared in this work have the same maneuver duration and maximum allowable input amplitudes, insofar as possible.

Similarly, $\mathcal{D}$ depends nonlinearly on the states via the sensitivity equations (11–13). Usually, the states are also outputs, and so output amplitudes must be comparable if an input design comparison is to be focused only on the merits of the input forms. For this reason, as well as to ensure validity of the assumed model structure, the inputs were designed to produce comparable output amplitudes. If the maneuver duration, input amplitudes, and output amplitudes are not the same for all input designs being compared, it is possible to arrange matters so that almost any chosen input form will appear to be the best, based on a criterion function that depends on $\mathcal{D}$.

For the optimal input design, the flight-test maneuver duration $T = N\Delta t$ was fixed a priori as a result of practical time constraints of the flight test and an analysis of the rate of decrease of the Cramér–Rao bounds with increasing maneuver time using the optimized input. The cost function to be minimized was the sum of squares of the Cramér–Rao bounds for the parameter standard errors:

$$J = \sum_{j=1}^{n_p} \sigma_j^2 = Tr[M^{-1}] = Tr[D] \tag{14}$$

for a given T. Another formulation of the cost can be defined to design the input for minimum flight-test time to achieve specific goals for the Cramér–Rao bounds.[14]

The optimal input applied to the dynamic system described by Eqs. (1–5) minimizes the cost function in Eq. (14), subject to the constraints in (6) and (7).

The optimization problem posed in the last paragraph is difficult to solve in general. For the particular problem of optimal input design for aircraft parameter estimation, there are good reasons to restrict the allowable input form to full amplitude square waves only. Among these are analytical work on a similar problem,[8] which indicated that the optimal input should be *bang-bang*, i.e., a full-amplitude switching input. Square wave inputs are simple to implement for either an onboard computer or the pilot. Finally, several flight test evaluations[11,12,16] have demonstrated that square wave inputs were superior to sinusoidal and doublet inputs for parameter estimation experiments, largely due to richer frequency spectra.

For the previously mentioned reasons, and to make the optimization problem tractable, input forms were limited to full-amplitude square waves only; i.e., only full positive, full negative, or zero amplitude was allowed for any input at any time. Full input amplitude was used to excite the system as much as possible. The choice of pulse timing and having zero amplitude available gave the optimizer the ability to use full input amplitudes without exceeding output amplitude constraints. With the preceding restrictions on the input form, the problem becomes a high-order combinatorial problem involving output amplitude constraints, which is well-suited to solution by the method of dynamic programming.

Dynamic programming is essentially a very efficient method for doing a global exhaustive search. Arbitrary dynamics such as control-surface actuator dynamics, feedback control, and general nonlinear models can therefore be included inside the optimization without difficulty. The result obtained is a globally optimal square wave input obtained in a single-pass solution. The technique includes provisions to adjust the input possibilities at certain times to account for practical limitations on frequency content of the input, such as avoiding structural resonance frequencies. The dynamic programming solution smoothly handles the multiple input problem, because this just changes the number of square wave input possibilities. Keeping the system responses within the output space for which the assumed model structure is valid can be handled directly with dynamic programming by discarding any input sequence whose output trajectory exceeds the constraint limits. The disadvantage of dynamic programming is the computational requirements, which expand rapidly with increasing n_i, n_s, n_o, n_p, or N. For aircraft parameter estimation problems, however, the computational cost is not prohibitive using current workstation computers. More details on the dynamic programming solution method can be found in Refs. 14 and 15.

Aircraft and Test Procedure

The F-18 High Alpha Research Vehicle (HARV) is a modified F/A-18 fighter.[19] The flight-test inputs were implemented by a computer-controlled on-board excitation system (OBES).

The pilot initiated each run by selecting a preprogrammed maneuver using buttons on a digital display interface (DDI) inside the cockpit. The aircraft was then brought to the desired trimmed flight condition and an engage/disengage button on the DDI was pressed to initiate the maneuver. Perturbation inputs were added directly to the appropriate control-surface actuator commands by the OBES, with the feedback control system still operating. The pilot held stick and rudder deflections constant at the trimmed values until the maneuver was complete. The maneuver could be disengaged manually by the pilot toggling the engage/disengage button, or automatically by the research flight control system, based on g limits, etc. The automatic flight control implemented for the flight-test maneuvers studied here was the NASA-1 control law in thrust vectoring (TV) mode.[20] Preprogrammed commands to the control-surface actuators were standard 3-2-1-1 inputs, doublets, or square wave inputs obtained from the optimal input design technique described earlier.

Various downlink data transmission rates were employed on the F-18 HARV aircraft, but all of the data used for analysis

was converted to a common sampling rate of 40 Hz. Corrections were applied to the angle of attack, sideslip angle, and linear accelerometer measurements to account for sensor offsets from the c.g., and the angle-of-attack measurement was corrected for upwash. Data compatibility analysis[21] revealed the need for a scale factor correction on the angle of attack and sideslip angle measurements from the wing-tip vane, and small bias error corrections on the measurements from the rate gyros and accelerometers.

Results

A priori linear models used for the input design were derived from a nonlinear batch simulation of the F-18 HARV,[22] which uses a wind tunnel database for the aerodynamics. Noise variance estimates for the input design were obtained from previous flight-test data records using an optimal Fourier smoothing technique.[23] The models used for parameter estimation from flight-test data were identical in structure to the a priori models, except that the a priori models did not include linear accelerometer outputs.

For lateral–directional aircraft dynamics, the state vector $\boldsymbol{x}$, input vector $\boldsymbol{u}$, and output vector $\boldsymbol{y}$ in Eqs. (1–4) are defined by

$$\boldsymbol{x} = [\beta\ p\ r\ \phi]^T, \qquad \boldsymbol{u} = [\delta r\ \delta a\ 1]^T \tag{15}$$

$$\boldsymbol{y} = [\beta\ p\ r\ \phi\ a_y]^T \tag{16}$$

System matrices A, B, C, and D contain the model parameters

$$A = \begin{bmatrix} Y_\beta & \sin\alpha_0 & -\cos\alpha_0 & (g/V_0)\cos\Theta_0 \\ L_\beta & L_p & L_r & 0 \\ N_\beta & N_p & N_r & 0 \\ 0 & 1 & \tan\Theta_0 & 0 \end{bmatrix}$$

$$B = \begin{bmatrix} Y_{\delta r} & Y_{\delta a} & Y_0 \\ L_{\delta r} & L_{\delta a} & L_0 \\ N_{\delta r} & N_{\delta a} & N_0 \\ 0 & 0 & 0 \end{bmatrix} \tag{17}$$

$$C = \begin{bmatrix} 1 & 0 & 0 & 0 \\ 0 & 1 & 0 & 0 \\ 0 & 0 & 1 & 0 \\ 0 & 0 & 0 & 1 \\ Y_\beta V_0/g & 0 & 0 & 0 \end{bmatrix}, \quad D = \begin{bmatrix} 0 & 0 & 0 \\ 0 & 0 & 0 \\ 0 & 0 & 0 \\ 0 & 0 & 0 \\ Y_{\delta r} V_0/g & Y_{\delta a} V_0/g & a_{y_0} \end{bmatrix} \tag{18}$$

For longitudinal short period aircraft dynamics

$$\boldsymbol{x} = [\alpha\ q]^T, \qquad \boldsymbol{u} = [\delta s\ 1]^T, \qquad \boldsymbol{y} = [\alpha\ q\ a_z]^T \tag{19}$$

System matrices containing the model parameters are

$$A = \begin{bmatrix} Z_\alpha & 1 + Z_q \\ M_\alpha & M_q \end{bmatrix}, \qquad B = \begin{bmatrix} Z_{\delta s} & Z_0 \\ M_{\delta s} & M_0 \end{bmatrix} \tag{20}$$

$$C = \begin{bmatrix} 1 & 0 \\ 0 & 1 \\ Z_\alpha V_0/g & Z_q V_0/g \end{bmatrix}, \qquad D = \begin{bmatrix} 0 & 0 \\ 0 & 0 \\ Z_{\delta s} V_0/g & a_{z_0} \end{bmatrix} \tag{21}$$

The data analysis was done using output error maximum likelihood parameter estimation in the time domain.[2,3] The data were analyzed as measured, not using perturbation quantities. The Cramér–Rao bounds for the parameter standard errors were computed from the square root of the diagonal elements of $\mathcal{D}$ from Eq. (9). Ordinarily, these values should be corrected for colored residuals.[3] The correction was not done here because the particular frequency content of the output residuals (usually from model structure errors) introduces a confounding factor in the comparison of data information content from different input forms. In the parameter estimation context, the estimated noise covariance matrix R used in Eq. (8) provides a measure of the mean square model fit error for all of the outputs, and this was considered appropriate for the present analysis. The model structure was the same for the compared maneuvers, so that the number of parameters estimated from each data record was identical. All data analysis and parameter estimates used radians for angular measure, but the plots were made using degrees.

The first input design was a lateral–directional case using the OBES to implement sequential rudder and aileron inputs. The flight condition was 5 deg angle of attack, Mach number 0.6, and an altitude of approximately 25,000 ft. The model was given by Eqs. (1–5) and (15–18). Input and output amplitude constraints were:

$$|\delta r| \le 4.0 \text{ deg}, \qquad |\delta a| \le 2.5 \text{ deg} \tag{22a}$$

$$|\beta| \le 5.0 \text{ deg}, \qquad |\phi| \le 32.0 \text{ deg} \tag{22b}$$

The 3-2-1-1 input form has been shown to be very effective for aircraft parameter estimation in previous flight-test investigations,[11,12] so this input was chosen to compare with the globally optimal square wave input design. To effect a fair comparison, the 3-2-1-1 and optimal inputs were designed using the same input amplitude constraints in Eq. (22a), the same maneuver duration, the same a priori model, and the same output amplitude constraints in (22b). Control-surface rate limits imposed for both input designs were 75 deg/s for the rudder and 100 deg/s for the aileron.

The 3-2-1-1 inputs were designed by matching the frequency of the "2" pulse to the frequency of the dominant oscillatory mode for the a priori model, and adjusting amplitudes and control sequence timing so that the output amplitude constraints were satisfied. Optimal inputs were designed with a computer program that implemented the optimal input design procedure described earlier.[14] Each maneuver lasted 24 s. For this case, the dynamic programming solution for the optimal square wave input required 19 MB of memory and took 108 min to run on a 200-MHz Sun Sparc Ultra 2.

The solid lines in Figs. 1a and 2a are the commanded OBES lateral–directional 3-2-1-1 and optimal inputs, and the dashed lines are the control-surface positions measured in flight. The desired input forms were distorted by the feedback control system, as can be seen in the figures. The distortion of the input forms by the lateral–directional feedback control system was not accounted for in the design process for either input design, because the distortion was expected to be small, based on a priori information about the control system. The input distortion that occurred can be considered equivalent to additional parametric error in the a priori linear model, because the input distortion was the result of a linear feedback control system. Figures 1 and 2 show that the maximum input and output amplitudes for these two maneuvers were very nearly the same, and the length of each maneuver was the same. The maneuvers were run in immediate succession on the same flight. With the model structure held fixed for the data analysis on each maneuver, any differences in the resulting model parameter accuracies can be attributed to the input form.

Parameter estimation results for the OBES lateral–directional 3-2-1-1 and optimal inputs at 5 deg angle of attack are given in Table 1. Column 1 in Table 1 lists the model parameters, column 2 contains the a priori values of the parameters used for the input design, and column 3 contains parameter estimates and Cramér–Rao lower bounds for the parameter standard errors using the 3-2-1-1 input. Column 4 contains the corresponding results for the optimal square wave input. The solid lines in Figs. 1b and 2b show measured outputs from flight. The dashed lines in Figs. 1b and 2b are the model responses computed using the measured inputs and the estimated

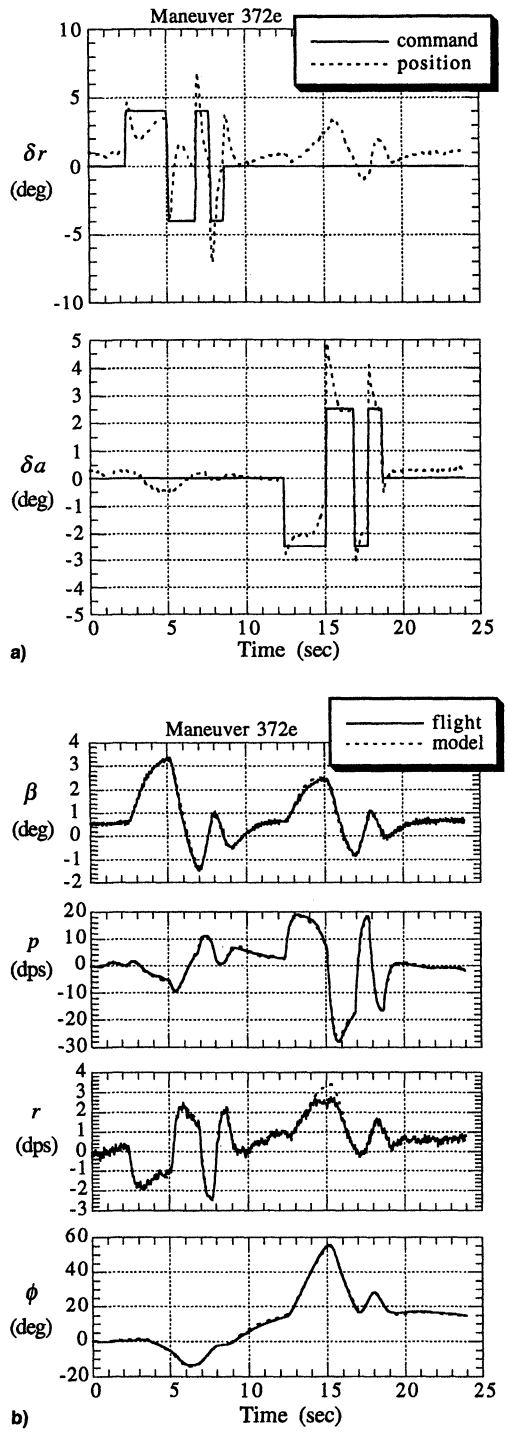

Fig. 1 Lateral–directional 3-2-1-1 input, 0.6/25 K, α = 5 deg.

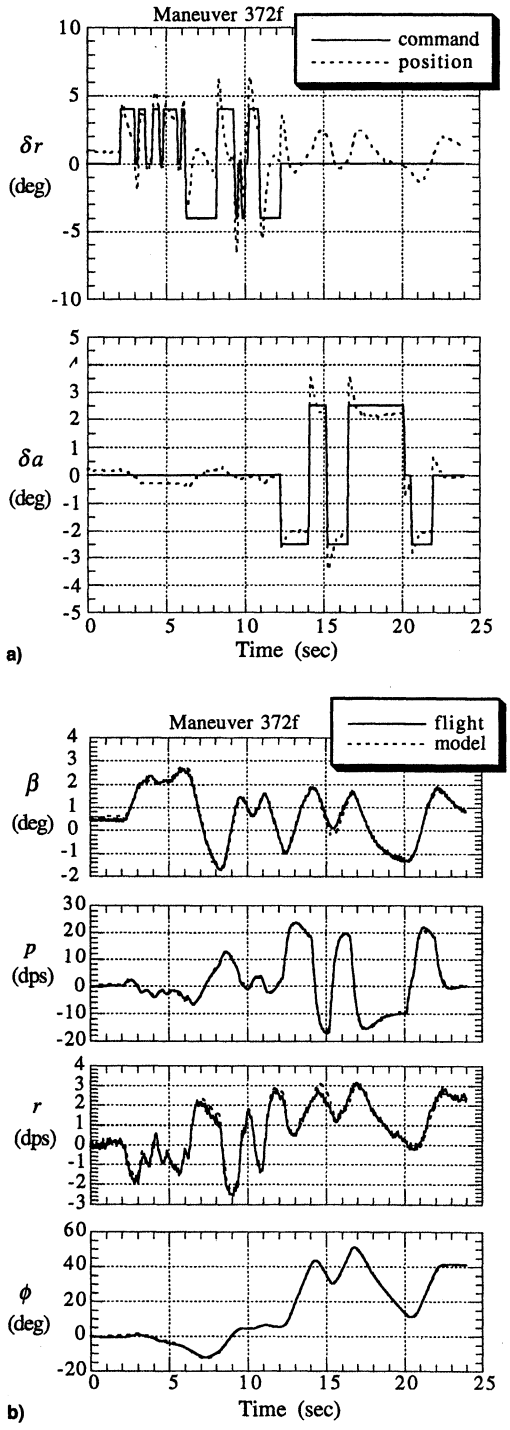

Fig. 2 Lateral–directional optimal input, 0.6/25 K, α = 5 deg.

model parameters from columns 3 and 4 of Table 1. The match is very good in both cases.

Values in column 5 of Table 1 are the percent change in the Cramér–Rao bound for each model parameter standard error for the optimal input maneuver compared to the 3-2-1-1 maneuver, based on the 3-2-1-1 value. The optimal input reduced parameter standard errors (equivalently, increased parameter accuracy) by an average 20%, with lower parameter standard errors for every estimated parameter. Parameter estimates in columns 3 and 4 of Table 1 are generally in good agreement.

The percent error of the a priori parameter values relative to the parameter values estimated from flight-test data (computed as the average of values in columns 3 and 4 of Table 1) varied from 4.2 to 65.1%, with an average value of 24.2%. This error in the a priori model parameters excludes the input distortion. Despite these errors, both input design methods based on the a priori model produced experimental data with excellent information content, as evidenced by the low standard errors in Table 1. As noted previously, the standard errors shown in Table 1 were not corrected for colored residuals because the proper corrections would be different for each parameter, depending on the coloring of the output residuals,[3] and this was viewed as a confounding factor for the input comparisons. In general, corrections for colored output residuals would increase the values given for the standard errors by a factor of 5–10.

Symmetric stabilator input designs implemented by OBES for longitudinal model identification are shown in Figs. 3 and 4. In this case, distortion of the input forms by the feedback

Table 1 Maximum likelihood results for lateral-directional OBES maneuvers[a]

Parameter	Estimate ± standard error: A priori estimate	3-2-1-1	Optimal	Standard error percent change
Y_β	−0.1316	−0.0970 ± 0.0013	−0.0859 ± 0.0012	−7.2
$Y_{\delta r}$	0.0285	0.0304 ± 0.0009	0.0327 ± 0.0008	−14.1
$Y_{\delta a}$	0.0053	0	0	——[b]
L_β	−11.56	−11.376 ± 0.048	−10.764 ± 0.037	−22.8
L_p	−1.592	−1.8120 ± 0.0070	−1.7998 ± 0.0055	−21.1
L_r	0.5462	0.3396 ± 0.0224	0.1727 ± 0.0200	−10.4
$L_{\delta r}$	1.910	2.3074 ± 0.0398	1.8768 ± 0.0316	−20.7
$L_{\delta a}$	−15.81	−19.480 ± 0.0623	−17.470 ± 0.0441	−29.3
N_β	2.139	1.2807 ± 0.0039	1.3120 ± 0.0028	−27.9
N_p	−0.0085	0	0	——[b]
N_r	−0.0940	−0.1027 ± 0.0021	−0.0436 ± 0.0019	−11.7
$N_{\delta r}$	−1.223	−1.3924 ± 0.0056	−1.3450 ± 0.0043	−23.5
$N_{\delta a}$	0.2444	0.1738 ± 0.0038	0.2383 ± 0.0028	−26.6

[a]F-18 HARV, 0.6/25 K, α = 5 deg.
[b]Parameter dropped in model structure determination.

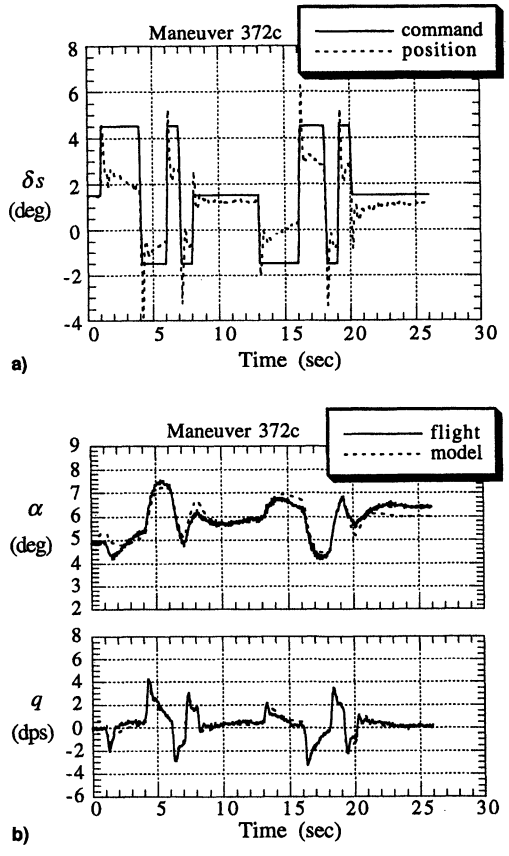

Fig. 3 Longitudinal 3-2-1-1 input, 0.6/25 K, α = 5 deg.

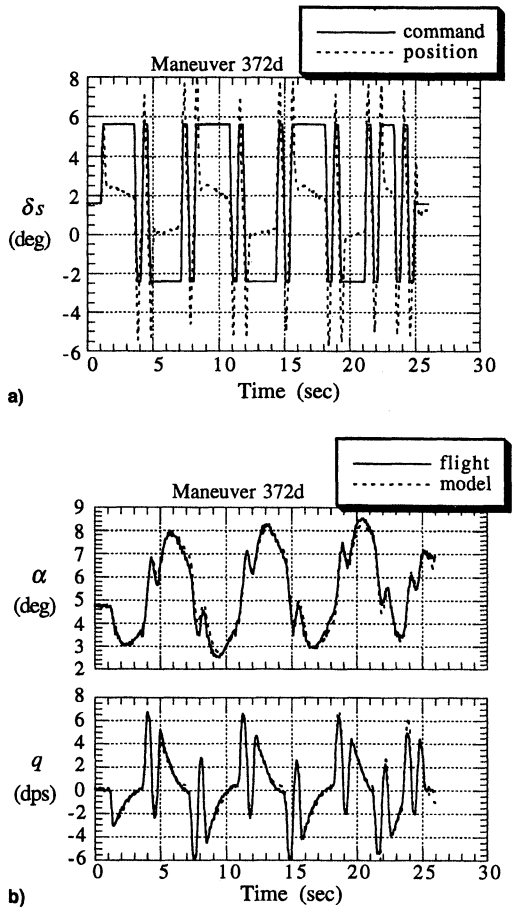

Fig. 4 Longitudinal optimal input, 0.6/25 K, α = 5 deg.

control was expected to be large, and was therefore accounted for in the a priori model by including a linear model of the feedback control identified from the nonlinear simulation. The same a priori model was used to design both inputs shown in Figs. 3 and 4, including a 40 deg/s rate limit on the stabilator deflection. The flight condition was again 5 deg angle of attack and Mach 0.6, with an altitude of approximately 25,000 ft. The model used for the parameter estimation is given by Eqs. (1–5) and (19–21). The same methods were used for the input designs and the data analysis, except that the optimal input design was allowed a higher input amplitude than the 3-2-1-1 input. This was done to investigate the capability available with the optimal input design routine to use higher input amplitudes for increased parameter accuracies while satisfying the same output amplitude constraints. Such flexibility is not available with the 3-2-1-1 input because of its fixed form. Perturbation input and output amplitude constraints were

$$|\delta s - \delta s_0| \leq 3.0 \text{ deg}, \quad \text{for the 3-2-1-1 input} \tag{23a}$$

$$|\delta s - \delta s_0| \leq 4.0 \text{ deg}, \quad \text{for the optimal input} \tag{23b}$$

$$|\alpha - \alpha_0| \leq 3.0 \text{ deg} \tag{23c}$$

Each maneuver lasted 26 s, and the maneuvers were run in immediate succession on the same flight. The dynamic programming solution for the optimal input required 19 MB of memory and took 52 min to run on a 200-MHz Sun Sparc

Table 2 Maximum likelihood results for longitudinal OBES maneuvers[a]

Parameter	Estimate ± standard error			
	A priori estimate	3-2-1-1	Optimal	Standard error percent change
Z_α	−0.5832	−0.5940 ± 0.0126	−0.6050 ± 0.0047	−62.8
Z_q	0	0	0	—[b]
$Z_{\delta s}$	−0.1093	−0.0378 ± 0.0063	−0.0789 ± 0.0032	−49.3
M_α	−2.2600	−4.543 ± 0.080	−2.195 ± 0.012	−85.1
M_q	−0.2927	−4.746 ± 0.109	−1.341 ± 0.014	−86.8
$M_{\delta s}$	−6.0380	−5.482 ± 0.104	−4.597 ± 0.024	−76.4

[a]F-18 HARV, 0.6/25 K, α = 5 deg.
[b]Parameter dropped in model structure determination.

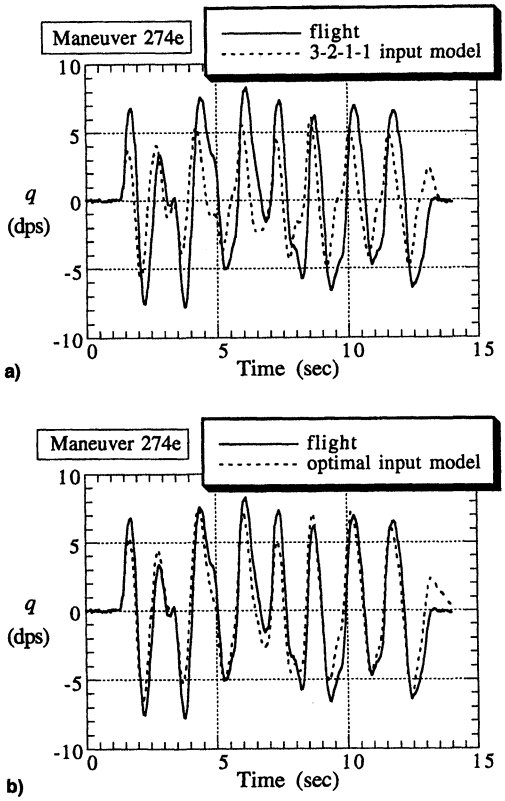

Fig. 5 Longitudinal prediction case, 0.6/25 K, α = 5 deg.

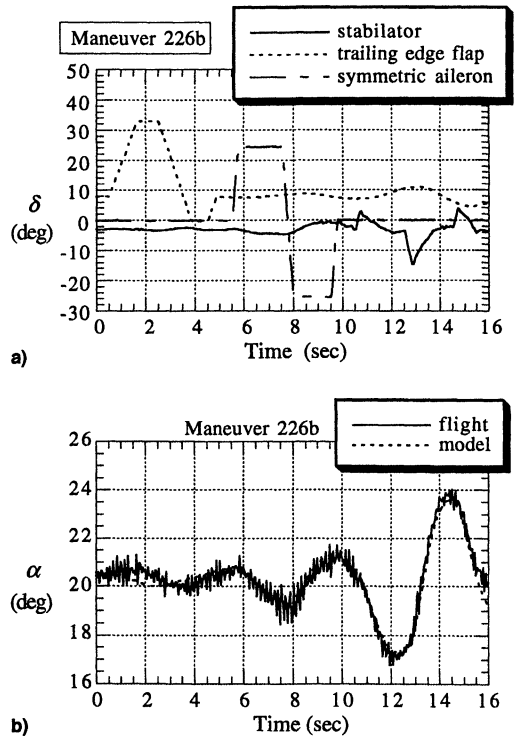

Fig. 6 Longitudinal doublet input, 0.35/25 K, α = 20 deg.

Ultra 2. Figures 3a and 4a show the significant distortion of the stabilator commands resulting from the longitudinal feedback control. Parameter estimation results are given in Table 2 using the same format as for Table 1. The parameter accuracies are now improved by an average 72%, using the optimal input compared with the 3-2-1-1 input. The optimal input maneuver produced larger α perturbations than the 3-2-1-1, although maximum α amplitude was the same for both inputs in the design phase using the a priori model. The reason for this discrepancy was that the control law removed most of the "3" pulse for the 3-2-1-1, and this effect was not well modeled in the a priori model. The optimal input used shorter pulses in general, and thus was less affected by this than the 3-2-1-1. Figures 3b and 4b indicate a good match between the measured outputs and the identified model responses using the measured inputs and the estimated model parameters from columns 3 and 4 of Table 2. Estimates of important pitching moment parameters in columns 3 and 4 of Table 2 do not agree well. Lower parameter standard error bounds for the optimal input indicate that the pitching moment parameter estimates from the optimal input should be more accurate. To check this, a different maneuver at the same flight condition was used to investigate the prediction capability of the models using the parameters in Table 2. Figure 5 shows measured and predicted pitch rate response using the model parameters from Table 2 with the same model structure used before. The stabilator input (not shown) was a perturbation input with an amplitude approximately ±5 deg from the trim value of 2 deg. The stabilator input was applied to both models to produce the prediction responses plotted with the measured response in Fig. 5. The prediction using the parameters estimated from the 3-2-1-1 input (shown in Fig. 5a) was less accurate than the prediction using the parameters from the optimal input (shown in Fig. 5b), both in frequency and amplitude. This result gives confidence that the parameters estimated from the optimal input maneuver are in fact more accurate, as indicated by the computed Cramér–Rao bounds.

Finally, two longitudinal maneuvers flown at 20 deg angle of attack, Mach 0.35, and approximately 25,000 ft altitude were studied to compare the optimal square wave input design with a sequence of doublets. Each maneuver lasted 16 s. The dynamic programming solution for the optimal input required 19 MB of memory and took 21 min to run on a 200-MHz Sun Sparc Ultra 2. Figure 6a shows the control-surface deflections for the doublet sequence. Individual doublets were commanded for the trailing-edge flap, symmetric aileron, and stabilator, in sequence. The traces in Fig. 6a are the measured control surface deflections, which include the effect of the feedback control system. The optimal input design used only the stabilator. Figure 7a shows measured stabilator deflection

Table 3 Maximum likelihood results for longitudinal OBES maneuvers[a]

Parameter	Estimate ± standard error		
	Doublets	Optimal	Standard error percent change
C_{Z_α}	−3.104 ± 0.143	−2.087 ± 0.066	−53.5
C_{Z_q}	−45.17 ± 6.91	−71.58 ± 3.72	−46.1
$C_{Z_{\delta f}}$	−0.4422 ± 0.0165	——[b]	——[b]
$C_{Z_{\delta a\ sym}}$	−0.2243 ± 0.0138	——[b]	——[b]
$C_{Z_{\delta s}}$	−0.7783 ± 0.1002	−0.8846 ± 0.0400	−60.0
C_{M_α}	−0.1792 ± 0.0179	−0.3313 ± 0.0037	−79.3
C_{M_q}	−54.08 ± 1.14	−16.10 ± 0.31	−72.4
$C_{M_{\delta f}}$	——[c]	——[b]	——[b]
$C_{M_{\delta a\ sym}}$	−0.0953 ± 0.0019	——[b]	——[b]
$C_{M_{\delta s}}$	−1.159 ± 0.019	−0.646 ± 0.005	−71.4

[a]F-18 HARV, 0.35/25 K, α = 20 deg. [b]Control not used. [c]Parameter dropped in model structcure determination.

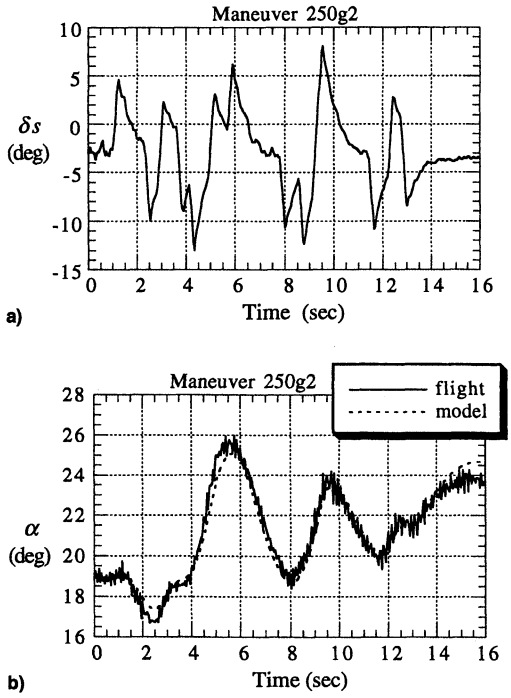

Fig. 7 Longitudinal optimal input, 0.35/25 K, α = 20 deg.

for the optimal square wave input, which was also distorted by the feedback control. The two maneuvers were run on different flights on different days, and so the data analysis was done using nondimensional stability and control derivatives. The model structure was the same as in the last example, except that the C_{Z_q} parameter was included for this higher angle-of-attack flight condition, and extra control derivatives were included for the doublet sequence maneuver because three controls were used. The additional controls put the doublet sequence maneuver at a disadvantage in the comparison because of the additional parameters to be estimated from the data record. This disadvantage was offset somewhat by the wider variety of excitation capability available using different control effectors. The stabilator perturbations from trim were approximately the same for the two maneuvers. An imprecise initial trim caused the nominal angle of attack to drift throughout the optimal input maneuver in Fig. 7. Figures 6b and 7b show that the maneuvers produced roughly the same magnitude of angle-of-attack perturbations and that the model matched the measurements very well for both maneuvers. Table 3 gives the results of the data analysis in a format similar to the other tables. The results indicate that the optimal input maneuver lowered the estimated parameter standard errors by an average 64% compared with the doublet sequence maneuver.

Concluding Remarks

The expense associated with flight testing modern aircraft dictates that flight-test data for modeling purposes be collected as efficiently as possible. In this work, the impact of input form on estimated parameter accuracy was investigated for three input design techniques: 3-2-1-1, doublets, and the optimal square wave. The tests were conducted on the F-18 HARV at 5 and 20 deg trim angles of attack. Comparisons were done on an equal basis, and it was found that the optimal input decreased estimated parameter standard errors (equivalently, increased estimated parameter accuracy) by an average of 20% compared with the 3-2-1-1 input for a lateral–directional case at 5 deg angle of attack. The decrease in estimated parameter standard errors improved to an average 72% for a longitudinal case at the same flight condition using higher input amplitudes in the optimal input design. Compared to a doublet sequence, the optimal input decreased estimated parameter standard errors by an average 64% for a longitudinal case at 20 deg angle of attack. For all comparisons, every individual parameter was estimated more accurately using the optimal square wave input.

The results of this investigation indicate that a properly designed 3-2-1-1 input can give good performance relative to the optimal square wave. Optimal square wave input designs demonstrated increased data information content in all cases studied, but the optimal input design technique is perhaps more valuable because of its ability to address practical design issues. Examples include an automated ability to limit output amplitude excursions during the flight-test maneuver, multiple input design capability, good robustness to errors in the a priori model and to distortions in the input form, and the design flexibility to investigate the impact of changes in the conditions or constraints of the input design, such as available maneuver time, control-surface rate limits, or I/O amplitude constraints. Such changes can be evaluated in terms of estimated parameter accuracies, using the single-pass global optimizer imbedded in the optimal input design procedure. Some of these capabilities were demonstrated in this work using flight-test results.

Acknowledgments

Discussions with Vladislav Klein of George Washington University contributed to the work presented here. Useful technical reviews were provided by Don Riley and Pat Murphy of NASA Langley Research Center. Flight tests were carried out at NASA Dryden Flight Research Center.

References

[1]Williams, J. N., Ham, J. A., and Tischler, M. B., "Flight Test Manual, Rotorcraft Frequency Domain Flight Testing," U.S. Army

Aviation Technical Test Center, AQTD Project 93-14, Edwards AFB, CA, Sept. 1995.

[2]Maine, R. E., and Iliff, K. W., "Application of Parameter Estimation to Aircraft Stability and Control—The Output-Error Approach," NASA RP 1168, June 1986.

[3]Morelli, E. A., and Klein, V., "Determining the Accuracy of Maximum Likelihood Parameter Estimates with Colored Residuals," NASA CR 194893, March 1994.

[4]Stepner, D. E., and Mehra, R. K., "Maximum Likelihood Identification and Optimal Input Design for Identifying Aircraft Stability and Control Derivatives," NASA CR 2200, March 1973.

[5]Mehra, R. K., "Optimal Input Signals for Parameter Estimation in Dynamic Systems—Survey and New Results," *IEEE Transactions on Automatic Control*, Vol. AC-19, No. 6, 1974, pp. 753–768.

[6]Gupta, N. K., and Hall, W. E., Jr., "Input Design for Identification of Aircraft Stability and Control Derivatives," NASA CR 2493, Feb. 1975.

[7]Mehra, R. K., and Gupta, N. K., "Status of Input Design for Aircraft Parameter Identification," *Methods for Aircraft State and Parameter Identification*, AGARD, CP 172, May 1975 (Paper 12).

[8]Chen, R. T. N., "Input Design for Aircraft Parameter Identification: Using Time-Optimal Control Formulation," *Methods for Aircraft State and Parameter Identification*, AGARD, CP 172, May 1975 (Paper 13).

[9]Gupta, N. K., and Hall, W. E., Jr., "Model Structure Determination and Test Input Selection for Identification of Nonlinear Regimes," Office of Naval Research, Rept. ONR-CR215-213-5, Arlington, VA, Feb. 1976.

[10]Gupta, N. K., Mehra, R. K., and Hall, W. E., Jr., "Application of Optimal Input Synthesis to Aircraft Parameter Identification," *Journal of Dynamic Systems, Measurement and Control*, Vol. 98, No. 2, 1976, pp. 139–145.

[11]Plaetschke, E., and Schulz, G., "Practical Input Signal Design," *Parameter Identification*, AGARD, Lecture Series No. 104, Nov. 1979 (Paper 3).

[12]Plaetschke, E., Mulder, J. A., and Breeman, J. H., "Flight Test Results of Five Input Signals for Aircraft Parameter Identification," *Proceedings of the 6th IFAC Symposium on Identification and System Parameter Estimation*, Vol. 2, Pergamon, 1982, pp. 1149–1154.

[13]Mulder, J. A., Sridhar, J. K., and Breeman, J. H., "Identification of Dynamic Systems—Applications to Aircraft, Part 2: Nonlinear Analysis and Manoeuvre Design," AGARD, AG-300, Vol. 3, Pt. 2, Neuilly Sur Seine, France, May 1994.

[14]Morelli, E. A., "Practical Input Optimization for Aircraft Parameter Estimation Experiments," NASA CR 191242, May 1993.

[15]Morelli, E. A., and Klein, V., "Optimal Input Design for Aircraft Parameter Estimation Using Dynamic Programming Principles," AIAA Paper 90-2801, Aug. 1990.

[16]Morelli, E. A., "Flight Test Validation of Optimal Input Design Using Pilot Implementation," *Proceedings of the 10th IFAC Symposium on System Identification*, Vol. 3, Danish Automation Society, Copenhagen, Denmark, 1994, pp. 43–48.

[17]Morelli, E. A., "Optimal Input Design for Closed Loop Modeling at High Angles of Attack," AIAA Paper 96-3418, July 1996.

[18]Van der Linden, C. A. A. M., Mulder, J. A., and Sridhar, J. K., "Recent Developments in Aircraft Parameter Identification at Delft University of Technology—Optimal Input Design," *Aerospace Vehicle Dynamics and Control*, Clarendon, Oxford, England, UK, 1994, pp. 259–284.

[19]Regenie, V., Gatlin, D., Kempel, R., and Matheny, N., "The F-18 High Alpha Research Vehicle: A High-Angle-of-Attack Testbed Aircraft," NASA TM 104253, Sept. 1992.

[20]HARV Control Law Design Team, "Design Specification for a Thrust-Vectoring, Actuated-Nose-Strake Flight Control Law for the High-Alpha Research Vehicle," NASA TM 110217, Nov. 1995.

[21]Klein, V., and Morgan, D. R. "Estimation of Bias Errors in Measured Airplane Responses Using Maximum Likelihood Method," NASA TM 89059, Jan. 1987.

[22]Messina, M., Strickland, M. E., Hoffler, K. D., Carzoo, S. W., Bundick, W. T., Yeager, J. C., and Beissner, F. L., Jr., "Simulation Model of the F/A-18 High Angle-of-Attack Research Vehicle Utilized for the Design of Advanced Control Laws," NASA TM 110216, May 1996.

[23]Morelli, E. A., "Estimating Noise Characteristics from Flight Test Data Using Optimal Fourier Smoothing," *Journal of Aircraft*, Vol. 32, No. 4, 1995, pp. 689–695.